

^{57}Fe Mössbauer study of high-valent Fe ions in Fe-substituted Li_2MnO_3

Yasuhiro Kobayashi¹ · Mitsuharu Tabuchi² · Makoto Seto¹

Published online: 08 June 2020
© Springer Nature Switzerland AG 2020

Abstract

The valence of Fe is important not only for chemical properties but also for magnetism and catalytic activity and so on. Fe substituted Li_2MnO_3 is known as a novel positive electrode material for high-capacity Li-ion battery. In the study of this material, high-valent (4+ or over) Fe ions were observed. In the previous studies, most of such high-valent Fe ions had been observed in the octahedral site of perovskite structure, for example, SrFeO_3 . However, Li_2MnO_3 has a rock-salt related structure. To elucidate the origin of this high-valent Fe, we observed ^{57}Fe Mössbauer spectroscopy of $\text{Li}_{1+x}(\text{Fe}_{0.2}\text{Mn}_{0.8})_{1-x}\text{O}_2$. The Mössbauer spectra measured at 3 K contained magnetic Fe^{4+} and Fe^{5+} . The area ratios of these components in the sample calcined in oxide were larger than those in the sample calcined in nitrogen. This result did not agree with the ratio of Fe sites obtained from X-ray diffraction. These high iron oxides are thought to be expressed by interaction with oxygen rather than site differences.

Keywords ^{57}Fe Mössbauer spectroscopy · High-valent Fe · Rock-salt structure

1 Introduction

The valence of Fe is important not only for chemical properties but also for magnetism and catalytic activity and so on. In simple iron oxides, such as Fe_2O_3 , Fe_3O_4 , and FeO , the oxidation numbers of irons are Fe^{2+} – Fe^{3+} . On the other hand, irons have a higher oxidation number in alkaline, alkaline-earth, and rare-earth-iron oxide. In SrFeO_3 and CaFeO_3 with a perovskite structure, the presence of Fe^{4+} is known, and these high iron oxides exist at the

This article is part of the Topical Collection on *Proceedings of the International Conference on the Applications of the Mössbauer Effect (ICAME2019), 1-6 September 2019, Dalian, China*
Edited by Tao Zhang, Junhu Wang and Xiaodong Wang

✉ Yasuhiro Kobayashi
ykoba@rri.kyoto-u.ac.jp

¹ Institute for Integrated Radiation and Nuclear Science, Kyoto University, 2, Asashiro-nishi, Kumatori, Osaka 590-0494, Japan

² National Institute of Advanced Industrial Science and Technology (AIST), 1-8-31, Midorigaoka, Ikeda, Osaka 563-7577, Japan

octahedral site [1]. Na_4FeO_4 has Fe^{4+} at the tetrahedral site [2]. As for Fe^{5+} , there is a report about $\text{La}_2\text{LiFeO}_6$, which exists at the octahedral site [3].

Fe^{4+} has been reported in Li and transition metal (TM) oxides doped with Fe in rock salt structure, and Fe^{4+} in tetrahedral site has been reported in $\text{Li}_{1-\delta}\text{Co}_{0.8}\text{Fe}_{0.2}\text{O}_2$ [4], $\text{Li}_{1.2-\delta}\text{Ti}_{0.4}\text{Fe}_{0.4}\text{O}_2$ [5], $\text{Li}_{1+x-\delta}(\text{Fe}_{0.25}\text{Mn}_{0.75})_{1-x}\text{O}_2$ [6] ($0 < x < 1/3$, $0 < \delta < 1$) and so on. In the past, Tabuchi et al. have reported the presence of Fe^{4+} and Fe^{5+} in Li_2MnO_3 with 30% iron substitution ($\text{Li}_{1+x}(\text{Fe}_{0.3}\text{Mn}_{0.7})_{1-x}\text{O}_2$) [7]. To investigate the details of these high iron oxide, we performed measurements on 20% iron-substituted Li_2MnO_3 , in which a higher concentration of high iron oxides was expected.

2 Experimental procedure

20% Fe-substituted Li_2MnO_3 ($\text{Li}_{1+x}(\text{Fe}_{0.2}\text{Mn}_{0.8})_{1-x}\text{O}_2$) is prepared by coprecipitation firing method. Fe-Mn mixed solution (Fe: Mn molar ratio = 2: 8) was prepared by dissolving $\text{Fe}(\text{NO}_3)_3 \cdot 9\text{H}_2\text{O}$ and $\text{MnCl}_2 \cdot 4\text{H}_2\text{O}$ in distilled water. The mixed solution was dropped into NaOH solution for 2–3 h to prepare Fe-Mn coprecipitate. The coprecipitate was wet oxidized by bubbling with O_2 for two days without removing residual alkaline. The aged product was washed with distilled water and filtered to remove residual alkaline and salts. The filtered product was mixed with LiOH solution ($\text{Li} / (\text{Mn} + \text{Fe}) = 2$) to make a uniform slurry, after which the slurry was dried at 50°C . The dried product was pulverized with a vibration mill. The Li-Fe-Mn mixed powder was first calcined at 500°C for 20 h in an O_2 atmosphere. After grinding on a vibration mill, the powder was finally calcined at 700 or 750°C for 20 h in O_2 or 750°C for 20 h in N_2 atmosphere. The three samples were named as samples 700-O, 750-O, and 750-N, respectively. After the final calcination, all samples were washed with distilled water to remove residual Li salt, and dried overnight at 100°C .

First, the samples were characterized by X-ray diffraction (XRD) analysis using an X-ray diffractometer (RINT TTR-III; Rigaku Corp.). In X-ray Rietveld analysis, software (RIETAN-FP [8]) was used to improve the structure. Si powder (SRM 640c; National Institute of Standards and Technology (NIST)) was used as an external standard. Transition metal occupancy (g) was refined using a constant isothermal oscillation coefficient (unity). The crystal structure is drawn by VESTA [9]. Li content was obtained by inductively coupled plasma (ICP) spectroscopy. The contents of Fe and Mn were obtained using a wavelength dispersive X-ray fluorescence spectrometer (Supermini200; Rigaku).

^{57}Fe Mössbauer measurements were performed at 3 to 300 K using the conventional Mössbauer spectrometer and the cryostat with helium refrigerator. 35 to 37 mg samples were mixed with boron nitride and pressed it into a 10 mm diameter pellet for Mössbauer transmission measurement. $\alpha\text{-Fe}$ was used for velocity calibration. The Mössbauer spectra were fitted with a MossWinn program [10, 11].

3 Results and discussion

Figure 1 shows the lattice structure of Li_2MnO_3 [12]. The colors (red and blue) indicate the occupancy of transition metal (TM) and Li at each site. Although the basic structure of this sample is a Li_2MnO_3 structure, the chemical formula of the sample is $\text{Li}_{1+x}(\text{Fe}_{0.2}\text{Mn}_{0.8})_{1-x}\text{O}_2$ due to the existence of defects and substitution of Li for TM. In this structure, Mn-Li layers

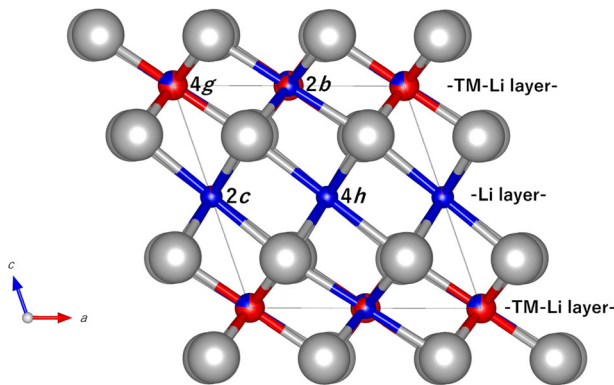


Fig. 1 Crystal structure of $\text{Li}_{1+x}(\text{Fe}_{0.2}\text{Mn}_{0.8})_{1-x}\text{O}_2$. The basic structure of this sample is a Li_2MnO_3 structure. The colors (red and blue) indicate the occupancy of transition metal (TM) and Li at each site, respectively. The gray-colored site is oxygen site

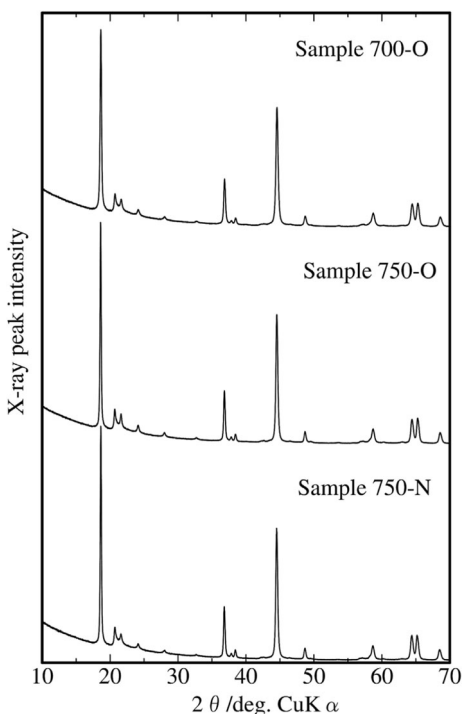
and Li layers are alternately stacked in the c -axis direction. All cations are present at the octahedral site. In the Mn-Li layer, Mn ions occupy 4 g sites to form a honeycomb lattice array, and Li ions occupy 2 b sites corresponding to the center position of each hexagon. There are two types of crystal sites, 2 c and 4 h , in the Li layer.

Figure 2 shows the X-ray diffraction patterns of the $\text{Li}_{1+x}(\text{Fe}_{0.2}\text{Mn}_{0.8})_{1-x}\text{O}_2$ samples at room temperature. Although the figure shows 10–70 degree patterns, we used 10–125 degree patterns for Rietveld analysis. All appearing peaks could be analyzed with a Li_2MnO_3 structure, and there are no impurities.

Table 1 shows the results of the Rietveld analysis. When comparing the data of sample 700-O to sample 750-O, almost same lattice parameters and lattice volumes (V) was observed. The g_{4g} value of sample 750-O was larger than sample 700-O. The g_{4g} is occupancy of the TM in the 4 g site. Moreover, the g_{2b} value of sample 750-O was smaller than sample 700-O. Therefore, the difference in $g_{4g}-g_{2b}$ value of sample 750-O was larger than that of sample 700-O. Since the value of $g_{4g}-g_{2b}$ corresponds to honeycomb lattice order parameter [13], sample 750-O has more honeycomb lattice regular structure than sample 700-O. Next, compare the structural data of sample 750-N with that of sample 750-O. The lattice parameters a , b , c , and lattice volume V of sample 750-N are larger than that of sample 750-O, suggesting that Fe or Mn ions were reduced by calcination in nitrogen. The $g_{4g}-g_{2b}$ value of sample 750-N is smaller than the $g_{4g}-g_{2b}$ value of sample 750-O. The fact shows that sample 750-N has less honeycomb lattice regular structure than sample 700-O. The g_{2c} and g_{4h} values for sample 750-N were less than 3%, as the values for sample 750-O.

Table 2 shows the $\text{Li} / (\text{Mn} + \text{Fe})$ and $\text{Fe} / (\text{Mn} + \text{Fe})$ ratios for samples 750-O and 750-N. The observed $\text{Fe} / (\text{Mn} + \text{Fe})$ ratio was slightly less than the nominal value of 0.20, but the difference in $\text{Fe} / (\text{Mn} + \text{Fe})$ ratio between samples is negligibly small. On the other hand, the $\text{Li} / (\text{Mn} + \text{Fe})$ ratio of sample 750-O was larger than that of sample 750-N. The fact corresponds to sample 750-O shifting to $\text{Li}_2\text{TM}^{4+}\text{O}_3$ side with $\text{LiTM}^{3+}\text{O}_2\text{-Li}_2\text{TM}^{4+}\text{O}_3$ solid solution compared to sample 750-N. This result suggests that the TM ions in sample 750-N are less valences than the TM ions in sample 750-O, as suggested by the XRD data. Furthermore, XANES results of similar samples indicate that the valence of Mn is tetravalent irrespective of the amount of Fe substitution [14]. Thus, the valence reduction of TM is owing to the valence of Fe. On the other hand, the decrease in Li ions is accompanied by a decrease in oxygen

Fig. 2 X-ray diffraction patterns of the $\text{Li}_{1+x}(\text{Fe}_{0.2}\text{Mn}_{0.8})_{1-x}\text{O}_2$ samples at room temperature



atoms, which means an increase in oxygen vacancies. This result is consistent with the difference in the calcination atmosphere.

Figure 3^(a) shows the Mössbauer spectra measured at 300 K are shown in Fig. 3 (a), and Table 3 shows the obtained parameters. The fitting model contains 2 or 3 doublets. Observed Mössbauer parameters in the samples 700-O and 750-O were similar. In XRD, the difference of the ordering in honeycomb structure was observed, but on the Mössbauer spectra, it did not appear clearly. From the IS values, component 1 can be assigned as high-spin Fe^{3+} , and the component 2 and 3 can be assigned as Fe^{4+} , respectively based on the previous data of electrochemically delithiated $\text{LiNi}_{0.90}\text{Fe}_{0.10}\text{O}_2$ [15]. The area ratios of Fe^{4+} components of samples 700-O and 750-O were larger than that of sample 750-N. The results indicate that Fe ion was more oxidized for samples 700-O and 750-O and agreed with smaller lattice parameters and volumes for both samples compared with those for sample 750-N. The result explains the chemical analysis data: the sample 750-O shift to $\text{Li}_2\text{TM}^{4+}\text{O}_3$ side on $\text{LiTM}^{3+}\text{O}_2 - \text{Li}_2\text{TM}^{4+}\text{O}_3$ solid solution compared to sample 750-N by oxidation of Fe ion.

Figure 3^(b) shows the Mössbauer spectra at 3 K. The fitting model consisted of three sextets and one singlet. In the largest sextet (component 1), a Gaussian function type distribution of the internal magnetic field is assumed. This distribution is thought to be due to the random arrangement of Fe and Mn. As listed in Table 3, component 1 and component 3 can be assigned as Fe^{3+} and Fe^{4+} based on IS value of $\alpha\text{-LiFeO}_2$ (+0.50 mm/s) [16] and SrFeO_3 (+0.154 mm/s) [1] at 4.2 K. The IS and internal field (H_{int}) for component 2 can be assigned as magnetic ordered pentavalent Fe ion on the octahedral site from the report of $\text{La}_2\text{LiFeO}_6$ (IS = -0.34 mm/s and $H_{\text{int}} = 23.6(2)$ T) at 4.2 K [3]. Surprisingly, the pentavalent ion can exist for sample 750-N which having the fewest amount of high valence Fe ion. From the IS value of

Table 1 X-ray Rietveld analysis data for all $\text{Li}_{1-x}(\text{Fe}_{0.2}\text{Mn}_{0.8})_{1-x}\text{O}_2$ samples using a monoclinic Li_2MnO_3 unit-cell ($C2/m$)

Sample	$a/\text{\AA}$	$b/\text{\AA}$	$c/\text{\AA}$	$\beta/\text{deg.}$	$V/\text{\AA}^3$	g_{4g}	g_{2b}	$g_{4g}\text{-}g_{2b}$	g_{2c}	g_{4h}
700-O	4.9466(6)	8.5580(8)	5.0261(5)	109.247(9)	200.9(6)	0.760(4)	0.336(3)	0.424(4)	0.028(3)	0.004(2)
750-O	4.9468(5)	8.5587(6)	5.0280(5)	109.274(7)	200.9(5)	0.802(3)	0.319(3)	0.483(3)	0.015(2)	0.0202(19)
750-N	4.9561(6)	8.5722(8)	5.0314(5)	109.237(8)	201.8(6)	0.777(4)	0.367(3)	0.410(4)	0.028(3)	0.014(2)

Table 2 Elemental analysis data for two $\text{Li}_{1+x}(\text{Fe}_{0.2}\text{Mn}_{0.8})_{1-x}\text{O}_2$ samples

Sample	Li/(Fe + Mn)	Fe/(Fe + Mn)
750-O	1.68(1)	0.185(1)
750-N	1.59(2)	0.184(1)

component 4, the component can be assigned also as Fe^{4+} [1]. The area ratios of Fe^{3+} components were similar to those for the doublet component at 300 K. At present, Fe^{5+} formed only a magnetic ordered state which is different observation from $\text{Li}_{1+x}(\text{Fe}_{0.3}\text{Mn}_{0.7})_{1-x}\text{O}_2$ reported previously [7]. In ref. [7], only paramagnetic Fe^{5+} component was detected at 5 K. The fact is different from typical pentavalent oxide, $\text{La}_2\text{LiFeO}_6$ [3].

It can be expected that the component 1 occupying the largest area in the Mössbauer spectra is the component from Fe in the 4 g site which is a stable position of TM. Moreover, it is natural to think about assigning components 2–4 to other sites. However, this assumption fails on sample 750-N. The component ratio of the Mössbauer spectra of sample 750-N is greatly different from other spectra at 300 K and 3 K. However, the change in the g value at each site determined by XRD is quite small. The area ratios of the Mössbauer spectra do not match the site ratio by the XRD. This result shows that the origin of Fe^{4+} and Fe^{5+} is not the specific crystal site that is shown in Table 1. We consider that the origin of the high-valent Fe ions are the interaction with oxygen atoms. Sample 750-N includes more oxygen vacancies than 750-O, and the oxygen vacancies stabilizes the trivalent Fe. We consider that the Fe atoms which are not adjacent to oxygen vacancies become the high-valent Fe. However, the positional relationship between Fe and oxygen vacancies has not been clarified in this study, therefore further research is needed for details.

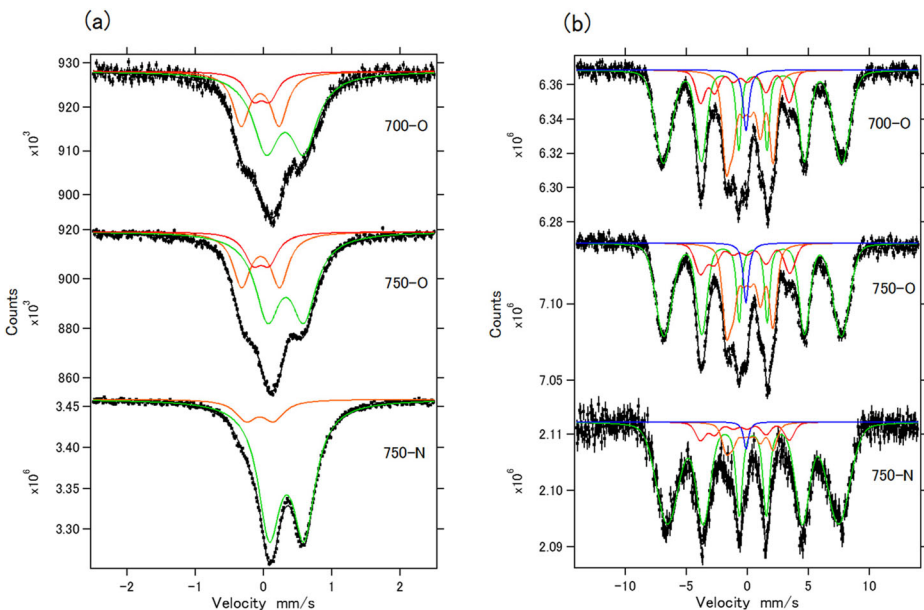


Fig. 3 Observed (closed square) and fitted ^{57}Fe Mössbauer spectra (black solid curve) at 300 K (a) and 3 K (b) for sample 700-O, 750-O, and 750-N. Green solid curves are component 1, red curves are component 2, orange curves are component 3, and blue curves are component 4

Table 3 ^{57}Fe Mössbauer analysis data for $\text{Li}_{1+x}(\text{Fe}_{0.2}\text{Mn}_{0.8})_{1-x}\text{O}_2$ samples. (* fixed parameters on the fitting)

Sample		300 K			3 K			
		Ratio	IS (mm/s)	QS (mm/s)	Ratio	IS (mm/s)	H_{in} (T)	QS (mm/s)
700-O	Component 1	60.7%	0.313	0.551	56.1%	0.439	45.4	-0.021
	Component 2	12.6%	-0.029	0.238	11.9%	-0.397	22.6	0.366
	Component 3	27.7%	-0.051	0.556	27.7%	0.058	12.0	0.244
	Component 4				4.3%	-0.104		
750-O	Component 1	59.2%	0.324	0.531	56.9%	0.452	45.2	-0.038
	Component 2	13.9%	-0.036	0.238	12.9%	-0.390	22.8	0.400
	Component 3	26.9%	-0.043	0.556	26.3%	0.071	11.9	0.226
	Component 4				3.9%	-0.118		
750-N	Component 1	79.9%	0.343	0.535	81.6%	0.452	43.6	0.021
	Component 2	20.1%	0.032	0.494	7.3%	-0.397*	22.6*	0.366*
	Component 3				9.4%	0.058*	12.0*	0.244*
	Component 4				1.6%	-0.104*		

4 Conclusion

X-ray diffraction and Mössbauer spectrum measurement of 20% Fe-substituted LiMnO_2 ($\text{Li}_{1+x}(\text{Fe}_{0.2}\text{Mn}_{0.8})_{1-x}\text{O}_2$) calcined with oxygen or nitrogen were performed. In XRD, the changes of the lattice ordering in the Mn-Li layer due to differences of the calcination temperature were observed, but the changes were small and not seen on the Mössbauer spectra. The components by Fe^{4+} and Fe^{5+} were observed in the Mössbauer spectra observed at 3 K. Moreover, the ratio of the high iron oxide component became small in the nitrogen calcined sample. However, the Fe site ratio obtained from XRD does not show a large difference between calcination in oxygen and nitrogen, and the site ratio cannot explain the change in the Mössbauer spectra. These high-valent irons are not due to the differences of the site. It seems that interactions with oxygen atoms and oxygen vacancies play an important role.

References

1. Menil, F.: Systematic trends of the ^{57}Fe Mössbauer isomer shifts in (FeO_n) and (FeF_n) polyhedra. Evidence of a new correlation between the isomer shift and the inductive effect of the competing bond T-X ($\rightarrow \text{Fe}$) (where X is O or F and T any element with a formal positive charge). *J. Phys. Chem. Solids*. **46**, 763–789 (1985)
2. Jeannot, C., Malaman, B., Gerardin, R., Oulladiad, B.: Synthesis, crystal and magnetic structures of the sodium ferrate (IV) Na_4FeO_4 studied by neutron diffraction and Mössbauer techniques. *J. Solid State Chem.* **165**, 266–277 (2002)
3. Demazeau, G., Buffat, B., Menil, F., Founes, L., Pouchard, M., Dance, J., Fabritchnyi, P., Hagenmuller, P.: Characterization of six-coordinated iron (V) in an oxide lattice. *Mat. Res. Bull.* **16**, 1465–1472 (1981)
4. MacLaren, V.L., West, A.R., Tabuchi, M., Nakashima, A., Takahara, H., Kobayashi, H., Sakaebe, H., Kageyama, H., Hirano, A., Takeda, Y.: Study of the capacity fading mechanism for Fe-substituted LiCoO_2 positive electrode. *J. Electrochem. Soc.* **151**, A672 (2004)
5. Tabuchi, M., Nakashima, A., Shigemura, H., Ado, K., Kobayashi, H., Sakaebe, H., Tastumi, K., Kageyama, H., Nakamura, T., Kanno, R.: Fine $\text{Li}_{(4-x)/3}\text{Ti}_{(2-2x)/3}\text{Fe}_x\text{O}_2$ ($0.18 \leq x \leq 0.67$) powder with cubic rock-salt structure as a positive electrode material for rechargeable lithium batteries. *J. Mater. Chem.* **13**, 1747 (2003)
6. Tabuchi, M., Kageyama, H., Kubota, K., Shibuya, H., Doumae, K., Kanno, R.: Structural change during charge–discharge for iron substituted lithium manganese oxide. *J. Power Sources*. **318**, 18–25 (2016)

7. Tabuchi, M., Tatsumi, K., Morimoto, S., Saito, T., Ikeda, Y.: Stabilization of tetra- and pentavalent Fe ions in Fe-substituted Li_2MnO_3 with layered rock-salt structure. *J. Appl. Phys.* **104**, 043909 (2008)
8. Izumi, F., Momma, K.: Three-dimensional visualization in powder diffraction. *Solid State Phenom.* **130**, 15–20 (2007)
9. Momma, K., Izumi, F.: VESTA 3 for three-dimensional visualization of crystal, volumetric and morphology data. *J. Appl. Crystallogr.* **44**, 1272–1276 (2011)
10. Klencsar, Z., Kuzmann, E., Vertes, A.: User-friendly software for Mössbauer spectrum analysis. *J. Radioanal. Nucl. Chem.* **210**, 105–118 (1996)
11. MossWinn - Mossbauer spectrum analysis and database software. <http://www.mosswinn.com/english/index.html>. Accessed 21 August 2019
12. Strobel, P., Lambert-Andron, B.: Crystallographic and magnetic structure of Li_2MnO_3 . *J. Solid State Chem.* **75**, 90–98 (1988)
13. Tabuchi, M., Kitta, M., Shibuya, H., Doumae, K., Yuge, R., Narita, K., Tamura, N.: Structural analysis during activation and cycling for Fe- and Ni-substituted Li_2MnO_3 positive electrode material. *Electrochim. Acta.* **303**, 9–20 (2019)
14. Tabuchi, M., Nakashima, A., Shigemura, H., Ado, K., Kobayashi, H., Sakaebe, H., Kageyama, H., Nakamura, T., Kohzaki, M., Hirano, A., Kanno, R.: Synthesis, cation distribution, and electrochemical properties of Fe-substituted Li_2MnO_3 as a novel 4 V positive electrode material. *J. Electrochem. Soc.* **149**, A509–A524 (2002)
15. Prado, G., Rougier, A., Fournes, L., Delmas, C.: Electrochemical behavior of iron-substituted lithium nickelate. *J. Electrochem. Soc.* **147**, 2880 (2000)
16. Tabuchi, M., Tsutsui, S., Masquelier, C., Kanno, R., Ado, K., Matsubara, I., Nasu, S., Kageyama, H.: Effect of cation arrangement on the magnetic properties of lithium ferrites (LiFeO_2) prepared by hydrothermal reaction and post-annealing method. *J. Solid State Chem.* **140**, 159–167 (1998)

Publisher's note Springer Nature remains neutral with regard to jurisdictional claims in published maps and institutional affiliations.